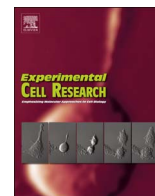




Contents lists available at ScienceDirect

Experimental Cell Research

journal homepage: [www.elsevier.com/locate/yexcr](http://www.elsevier.com/locate/yexcr)

## External $\text{Ca}^{2+}$ regulates polycystin-2 (TRPP2) cation currents in LLC-PK1 renal epithelial cells

Xiao Qing Dai<sup>a,1</sup>, Paula L. Perez<sup>c,1</sup>, Gonzalo Soria<sup>b</sup>, Noelia Scarinci<sup>c</sup>, Mariano Smoler<sup>c</sup>,  
D. Cristian Morsucci<sup>b</sup>, Kunimasa Suzuki<sup>d</sup>, María del Rocío Cantero<sup>c</sup>, Horacio F. Cantiello<sup>b,c,\*</sup>

<sup>a</sup> Alberta Diabetes Institute, Department of Pharmacology, University of Edmonton, Alberta, Canada

<sup>b</sup> Nephrology Division, Department of Medicine, Massachusetts General Hospital and Harvard Medical School, Charlestown, MA, USA

<sup>c</sup> Laboratorio de Canales Iónicos, CONICET, Cátedra de Biofísica y Bioestadística, Facultad de Odontología, UBA, Buenos Aires, Argentina

<sup>d</sup> Molecular Biology and Biochemistry Core Facility, Alberta Diabetes Institute, University of Alberta, Edmonton, Alberta, Canada

### ARTICLE INFO

#### Keywords:

TRP channels  
Polycystin-2  
TRPP2  
 $\text{Ca}^{2+}$  sensing receptor

### ABSTRACT

Polycystin-2 (PC2, TRPP2) is a nonselective cation channel whose dysfunction is associated with the onset of autosomal dominant polycystic kidney disease (ADPKD). PC2 contributes to  $\text{Ca}^{2+}$  transport and cell signaling in renal epithelia and other tissues. Little is known however, as to the external  $\text{Ca}^{2+}$  regulation of PC2 channel function. In this study, we explored the effect of external  $\text{Ca}^{2+}$  on endogenous PC2 in wild type LLC-PK1 renal epithelial cells. We obtained whole cell currents at different external  $\text{Ca}^{2+}$  concentrations, and observed that the basal whole cell conductance in normal  $\text{Ca}^{2+}$  (1.2 mM), decreased by 30.2% in zero (nominal)  $\text{Ca}^{2+}$  and conversely, increased by 38% in high external  $\text{Ca}^{2+}$  (6.2 mM). The high  $\text{Ca}^{2+}$ -increased whole cell currents were completely inhibited by either PC2 gene silencing, or intracellular dialysis with active, but not denatured by boiling, PC2 antibody. Exposure of cells to high  $\text{Ca}^{2+}$  was also associated with relocation of PC2 to the plasma membrane. To explore whether a  $\text{Ca}^{2+}$  sensing receptor (CaSR) was implicated in the external  $\text{Ca}^{2+}$  modulation of PC2 currents, we tested the effect of the CaSR agonists, spermine and the calcimimetic R-568, which largely mimicked the effect of high  $\text{Ca}^{2+}$  under  $\text{Ca}^{2+}$ -free conditions. The CaSR agonist gentamicin also increased the PC2 currents in the presence of normal  $\text{Ca}^{2+}$ . The presence of CaSR was confirmed by immunocytochemistry, which partially colocalized with the intracellular PC2 protein, in an external  $\text{Ca}^{2+}$ -dependent manner. The data support a novel  $\text{Ca}^{2+}$  sensing mechanism for PC2 expression and functional regulation in renal epithelial cells.

### 1. Introduction

PC2 is a member of the superfamily of TRP cation channels [23] that is encoded by the PKD2 gene, whose mutations are responsible for ADPKD [21]. PC2 is a  $\text{Ca}^{2+}$ -permeable nonselective cation channel [10,36] that is implicated in a number of cellular functions [9]. PC2 has been detected in different cellular locations [7], including the plasma membrane [18,25], the endoplasmic reticulum [15,25], and the primary cilium [2,14,29]. Ciliary located PC2 in particular, is reported to be one of the key elements in the mechano-sensory response of renal epithelia to fluid flow [24], whose integrity may prevent cyst formation [32]. Previous studies from our laboratory determined a functional PC2 in the primary cilium of LLC-PK1 cells [29], which is regulated by a ciliary located type-2 vasopressin receptor and the production of local cAMP [30]. This PC2 function may have a relevant role in ciliary  $\text{Ca}^{2+}$

transport, and the regulation of ciliary length. PC2 activation is also associated with a rise in cell  $\text{Ca}^{2+}$  [24], which may not be mediated by the ciliary PC2 but instead functional channels located in the plasma membrane. Thus,  $\text{Ca}^{2+}$  influx through a functional plasma membrane PC2 seems to be essential in normal cell responses. Little is known, however, as to the expression and function of endogenous PC2 to the plasma membrane, and how  $\text{Ca}^{2+}$ -dependent mechanisms may regulate this function. This is particularly evident from expected  $\text{Ca}^{2+}$  feedback signals entailing PC2-mediated  $\text{Ca}^{2+}$  transport that should depend on the availability of external  $\text{Ca}^{2+}$ . Recent studies from our laboratory, for example, determined that the isolated protein is not affected by extracellular  $\text{Ca}^{2+}$ , but instead to a feedback mechanism mediated by  $\text{Ca}^{2+}$  influx through the channel, and the regulatory binding of  $\text{Ca}^{2+}$  to putative intracellular cytoskeletal partners that are controlled by a local pool of  $\text{Ca}^{2+}$  [3]. PC2 regulatory mechanisms that

\* Correspondence to: Laboratorio de Canales Iónicos, CONICET, Cátedra de Biofísica y Bioestadística, Facultad de Odontología, UBA, Marcelo T. de Alvear 2142 16B, CABA 1122, Argentina.

E-mail address: [hcantiello@yahoo.com.ar](mailto:hcantiello@yahoo.com.ar) (H.F. Cantiello).

<sup>1</sup> Xiao Qing Dai and Paula L. Perez made equal contributions to the present study.

<http://dx.doi.org/10.1016/j.yexcr.2016.11.004>

Received 24 March 2016; Received in revised form 13 October 2016; Accepted 5 November 2016

Available online xxx

0014-4827/ © 2016 Published by Elsevier Inc.

may be associated with external  $\text{Ca}^{2+}$  concentrations still are heretofore largely unknown. The fact that PC2 itself does not respond to varying external  $\text{Ca}^{2+}$  concentrations [3], invokes the need for other sensing mechanisms of external  $\text{Ca}^{2+}$  regulation that may implicate putative “ $\text{Ca}^{2+}$  detectors” of extracellular  $\text{Ca}^{2+}$ . One such mechanism is the  $\text{Ca}^{2+}$ -sensing receptor (CaSR) [12,20] that responds to extracellular  $\text{Ca}^{2+}$  concentrations in the range of 0.5–10 mM, and has been observed in the various nephron sections of the mammalian kidney [12,31].

The aim of the present study was to assess whether changes in external  $\text{Ca}^{2+}$  concentration modify the whole cell conductance of wild type LLC-PK1 renal epithelial cells, and whether this contribution may be associated with endogenous PC2 function. Our data indicate that high external  $\text{Ca}^{2+}$  increased the whole cell conductance of LLC-PK1 cells particularly the stimulation of endogenous PC2-mediated currents, which were blocked either by silencing of the PKD2 gene, or intracellular dialysis with an active anti-PC2 antibody, raised against the carboxy-terminus of the channel protein. The stimulatory effect of high external  $\text{Ca}^{2+}$  on the PC2 currents, was mimicked by CaSR agonists, including spermine, and the calcimimetic R-568, in the absence of external  $\text{Ca}^{2+}$ , and gentamicin in the presence of normal  $\text{Ca}^{2+}$ . CaSR was identified by immunocytochemistry, and observed immuno-colocalized with the PC2 channel protein in a manner that depended on external  $\text{Ca}^{2+}$ . The encompassed data are consistent with a regulatory pathway where external  $\text{Ca}^{2+}$  modulates a  $\text{Ca}^{2+}$  sensing mechanism that effects PC2 regulation in LLC-PK1 renal epithelial cells. This regulatory mechanism may help explain the connection between  $\text{Ca}^{2+}$  signals and the onset of ADPKD.

## 2. Materials and methods

### 2.1. Cell culture

Wild-type LLC-PK1 cells were cultured as described [28], in Dulbecco's modified Eagle's medium (DMEM) supplemented with 10% fetal bovine serum (FBS), without antibiotics. Cells were grown at 37 °C, in a humidified atmosphere with 5%  $\text{CO}_2$  to reach partial confluence in two-to-three days. Islands of confluent cells and attached single cells were used for immunocytochemical and electrical studies, respectively.

### 2.2. Immunocytochemistry

Cells were grown on glass coverslips, rinsed twice with phosphate-buffered saline (PBS), and fixed for 10 min in freshly prepared solution of para-formaldehyde (4%) and sucrose (2%). Cells were washed three times with PBS, blocked for 30 min with BSA (1%) in PBS and then incubated for 60 min with specific anti-PC2 primary antibody. Two polyclonal anti-PC2 antibodies (0.2 mg/ml stock solution) were used in the present study. The antibody that binds to intracellular site was raised against a synthetic peptide sequence (871-ERAKLKRREVLGR-883) corresponding to amino acids 871–883 from the carboxy terminus of human PC2, obtained from PolyFast (Zymed Laboratories Inc., South San Francisco, CA) and used at 1:100 dilutions as previously reported [29]. This antibody and others raised against this domain of PC2 have shown strong inhibitory effect on PC2 single channel activity [3,10,29]. A second antibody raised to a recombinant fragment corresponding to amino acids 261–361 of human PC2 (PC2-Ab<sup>exep</sup>) representing an external domain of the protein was obtained from Abcam (ab 55600, Cambridge MA) and was used at a 1:100 dilution in non-permeabilized cells. The CaSR primary antibody was obtained from Novus Biologicals (NB120-19347, Littleton, CO, USA) and was used at a 1:1000 dilution. Secondary antibodies were the CY3 conjugated affinity purified donkey anti-mouse IgG from Jackson ImmunoResearch Labs (West Grove, PA), anti-rabbit IgG-FITC from Santa Cruz Biotechnology, Inc. (Santa Cruz, CA) and goat anti-mouse IgG-FITC from Invitrogen (Frederick, MD). Cells were also stained

with DAPI to visualize the nuclei, and also stained with FITC-phalloidin (Sigma-Aldrich, St. Louis, MO, USA) to label the actin cytoskeleton. Stained cells were mounted with Vectashield mounting medium (Vector Laboratories, Burlingame, CA) and viewed under an inverted Olympus IX71 microscope connected to a digital CCD camera C4742-80-12AG (Hamamatsu Photonics KK, Bridgewater, NJ). Images were collected with the IPLab Spectrum (Scanalytics, Viena, VA) acquisition and analysis software, running on a Dell-NEC personal computer. Final composite images were created using Adobe PhotoShop CS2 (Adobe systems, Inc., Newton, MA).

### 2.3. Cellular location of PC2 and CaSR

To assess the cellular location of PC2 under the various experimental conditions, islands of subconfluent LLC-PK1 cells were co-stained with anti-PC2 antibody (Red), FITC-phalloidin (Green), and DAPI (Blue), to label PC2, the actin cytoskeleton, and nuclei to calculate the number of cells in the cluster, respectively [27]. PC2 was identified as either diffuse perinuclear reddish staining, or bright punctuate (Red) staining. The latter one was further identified as being associated with plasma membrane PC2, by the colocalization with cortical cytoskeleton apposed to cell-to-cell contacts. The number of punctuate loci per cluster was counted and divided by the number of DAPI-stained nuclei. Data were expressed in arbitrary units (AU) per cell as representing the number of PC2 punctuate staining per cell in the cluster, for the various experimental conditions. CaSR was co-immunolocalized with PC2, utilizing specific primary antibodies, and FITC- (Green), and rhodamine- (Red) complexed secondary antibodies, respectively. Cells were counterstained with DAPI to locate cell nuclei. To quantify immuno-colocalized proteins, regions of interest (ROI) in each merged image were digitally analyzed with IPLab for Windows 4.0. Briefly, ROI were chosen to select oval areas roughly containing one cell each (as indicated by nuclear staining). Each ROI was further explored for either one of three possible filters, namely, Green for CaSR, Red for PC2, and Yellow, for the colocalized complex. Each color was quantified with the IPLab subroutine Measure Seg/ROI, and further made relative to 100% ROI staining, to eliminate potential differences in single channel brightness. Twenty to forty cells were counted for each external  $\text{Ca}^{2+}$  condition, from at least three different stained preparations, unless otherwise indicated. Data were averaged and expressed as the mean  $\pm$  SEM (n=number of cells used in the average), and compared by one-way ANOVA, establishing statistical significance at  $p < 0.05$  [34].

### 2.4. PKD2 gene silencing

Silencing of PKD2 gene expression in cultured LLC-PK1 cells was conducted using the small interfering RNA technique, as previously reported [37]. Two 21-nt PKD2-specific synthetic siRNAs, one of which was a fluorescent (fluorescein) probe, were synthesized by Invitrogen (Buenos Aires, Argentina), as well as a 19-nt irrelevant sequence as scrambled control (Ir-siRNA). All constructs bore dTdT overhangs at the 3' end, as originally reported [37]. The sense sequences of siRNAs were as follows; (siPKD2) GCUCCAGUGUGUACUACUACA, starting at 906 in exon 3 of the PKD2 gene, and (Ir-siRNA) UUCUCCGAACGUGUCACGU, as scrambled control.

### 2.5. siRNA transfection

For the siRNA transfection studies, cell cultures were trypsinized and placed at 70% confluence in 35-mm cell culture dishes containing DMEM supplemented with 3% FBS at 37 °C in a 5%  $\text{CO}_2$  atmosphere. The following day, transfection was performed with DharmaFECT1 (GE Healthcare; Ottawa, ON). Briefly, the protocol was as follows, two sets of tubes were prepared, one for siRNA and the other for Dharmafect. Tubes were added either 10  $\mu\text{l}$  of scrambled (Irss) or

antisense RNA (siPKD2) with 100  $\mu$ l Optimum medium, or 2  $\mu$ l of Dharmafect with 100  $\mu$ l Optimum medium. The second tube was incubated for 5 min at room temperature and then mixed with either scrambled or antisense RNA for another 20 min (200  $\mu$ l total volume). Incubation was conducted by medium change to the cell cultures with a mixture of fresh medium (800  $\mu$ l, DMEM plus 3% FBS), and 200  $\mu$ l of the transfection mixture. The total transfection time was three over-nights (72 h).

## 2.6. Real-time quantitative PCR analysis

Real-time quantitative PCR was conducted as previously reported [11]. Briefly, total RNA was extracted using TRIzol Reagent (Thermo Fisher/Life Technologies). The cDNA was generated using 1  $\mu$ g total RNA and 5x All-In-One RT Master Mix (Applied Biological Materials Inc., Richmond, BC, Canada). Real-time quantitative PCR assays were carried out in a 7900HT Fast Real-Time PCR system (Thermo Fisher/Applied Biosystems) using Fast SYBR Green Master Mix (Thermo Fisher/Applied Biosystems), 0.5  $\mu$ M primers and 50 ng cDNA. After an initial 30-s denaturation step at 95  $^{\circ}$ C, the cDNA was amplified by forty two-second cycles of denaturation at 95  $^{\circ}$ C, and extension at 60  $^{\circ}$ C for 20 s. Two sets of PCR primers, including the forward and reverse primers of porcine PKD2 or  $\beta$ 2-microglobulin ( $\beta$ 2MG) genes, are listed below:

PKD2 primer set.  
forward PKD2: 5'-CGTCTACTCCGTCAGCAGTGAGGACAG-3',  
reverse PKD2: 5'-GTTCTCGACAAATCCAGGTAATAGCCAGCTCC-3';  
 $\beta$ 2MG primer set.  
forward  $\beta$ 2MG: 5'-GCTCTCACTGTCTGGCCTGGATG-3',  
reverse  $\beta$ 2MG: 5'-GTTTCATCTTCTCCCGTTTTTCAGCAAATC-3'.

## 2.7. Western blotting technique

The silencing efficiency was confirmed by Western blot technique. Proteins were extracted from cells by cell lysis with a buffer solution containing Triton X100 and HEPES, and centrifugated for 20 min at 12,500 rpm in an Eppendorf 5414 microfuge in the cold. The Western blot technique was conducted as follows: Equal amounts of protein extracts were mixed with sample buffer and then separated on 10% SDS-PAGE gels (40  $\mu$ g/lane) for 100 min at constant 120 V and maximum current. The gel was then transferred to a nitrocellulose membrane, and the presence of proteins confirmed by staining with Ponceau Red. For immunodetection, the membrane was blocked for 1 h with 5% skim milk and incubated overnight with the primary anti PC2 antibody (1:500, Santa Cruz Biotechnology) at 4  $^{\circ}$ C. The membrane was washed with Tris-buffered saline and Tris buffered saline-Tween (TBST) and subsequently incubated with a secondary anti-rabbit antibody coupled with horseradish peroxidase (1:500, Promega). Specific labeling was detected by treatment with diaminobenzidine (DAB, Sigma Aldrich), resulting in a brown precipitate.

## 2.8. Reagents

All reagents were obtained, except otherwise indicated, from Sigma-Aldrich (St. Louis, MO, USA). Spermine tetrahydrochloride (S2876) was prepared in distilled water (100 mM), and used at a 2 mM final concentration. Gentamicin in distilled water (G1397, 50 mg/ml) was diluted to a final concentration of (250  $\mu$ g/ml) into the test solution at the time of the experiment. Ketamine hydrochloride (K4138) was used at a final concentration of 1  $\mu$ g/ml after dilution from an 80 mg/ml original solution. The calcimimetic CaSR agonist R-568 hydrochloride (SC-361302), was obtained from Santa Cruz Biotechnology Inc. (Santa Cruz, CA, USA), and was used at a final concentration of 5  $\mu$ M. Wherever indicated the anti PC2 antibody was used after inactivation by boiling the final solution containing a 1:50

dilution for 15 min.

## 2.9. Free $Ca^{2+}$ calculations and $Ca^{2+}$ chelation

To change the external  $Ca^{2+}$  concentration, the bathing solution containing nominal free  $Ca^{2+}$  was prepared as follows. The  $Ca^{2+}$  chelating agent EGTA (ethylene-bis(oxyethylenenitrilo) tetraacetic acid, 100 mM) was dissolved in NaOH and titrated with HCl to reach pH  $\sim$ 7.0, added at a 1 mM final concentration. The final  $Ca^{2+}$  concentration was calculated by:

$$[Ca] = \frac{K_Q[CaQ]}{[Q]}$$

where  $K_Q$  is the dissociation constant of the  $Ca^{2+}$ -chelator complex,  $[Q]$  is the concentration of the free chelating agent, and  $[CaQ]$  is the concentration of  $Ca^{2+}$  bound to  $Q$ . Calculations were corroborated by the free on-line site <http://maxchelator.stanford.edu/CaEGTA-TS.htm>. The nominal  $Ca^{2+}$  free solution was estimated to have a concentration of 0.32 nM. Whenever indicated,  $CaCl_2$  was added from a 500 mM stock solution to reach either free  $Ca^{2+}$  1.2 mM or 6.2 mM as indicated in Section 3. The solutions containing different external  $Ca^{2+}$  concentrations were labeled throughout the study as 0 Ca, 1.2 Ca, and 6.2 Ca, respectively.

## 2.10. Voltage clamp electrophysiology

The whole cell voltage clamping technique was conducted at room temperature as previously described [27]. Patch pipettes were pulled from KG-33 glass capillaries (Garner Glass, Claremont, CA) and filled with a solution containing (in mM): 140 KCl, 5 NaCl, 1.0 EGTA, and 10 HEPES (pH adjusted to 7.2 with N-methyl-d-glucamine). The bath solution contained (in mM): 135 NaCl, 5 KCl, 0.8  $MgSO_4$ , and 10 HEPES (pH adjusted to 7.4 with N-methyl-d-glucamine). Osmotic shock comparison was conducted by addition of 15 mM sucrose to the normal (1.2 mM  $Ca^{2+}$ ) solution. Please note that the osmolarities were as follows: the 0 Ca solution is 302.6 mOsm, the 1.2 Ca 305.2 mOsm, and the 6.2 Ca 320.2 mOsm. The sucrose supplemented solution was 320.2 mOsm. To obtain whole-cell current-voltage relationships, voltage protocols included trains of 20 mV voltage steps (400 ms) between  $\pm$  100 mV, from a holding potential of zero mV. The voltage clamp techniques was conducted with either a Dagan 3900 patch clamp amplifier (Dagan Corp., Minneapolis, MN) driven by pCLAMP Version 10.2 (Axon Instruments, Foster City, CA), or an EPC10 patch-clamp amplifier controlled with PatchMaster software (HEKA Elektronik, Lambrecht, Germany). The maximal whole cell conductance for a given condition was approximated as a linear fitting of the outward currents at positive holding potentials (+60 to +100 mV). Whole-cell currents were corrected by membrane capacitance approximated as exponential decay capacitive transients scaled and corrected by series resistance. Thus, whole cell current absolute values were expressed as pA/pF, while the whole-cell conductance was expressed in S/F. The reversal potential  $V_{rev}$  was calculated from experimental data as interpolation of the linear relationship between current data points near zero current and the holding potentials.

## 2.11. Statistical analysis

Statistical analysis and graphics were conducted with Sigmaplot Version 11.0 (Jandel Scientific, Corte Madera, CA). Statistical significance was obtained either by unpaired "t" test comparison of sample groups of similar size or one-way ANOVA [34]. Average data values were expressed as the mean  $\pm$  SEM for each condition, where "n" represents the number of cells analyzed. Statistical significance was accepted at  $p < 0.05$  [34].

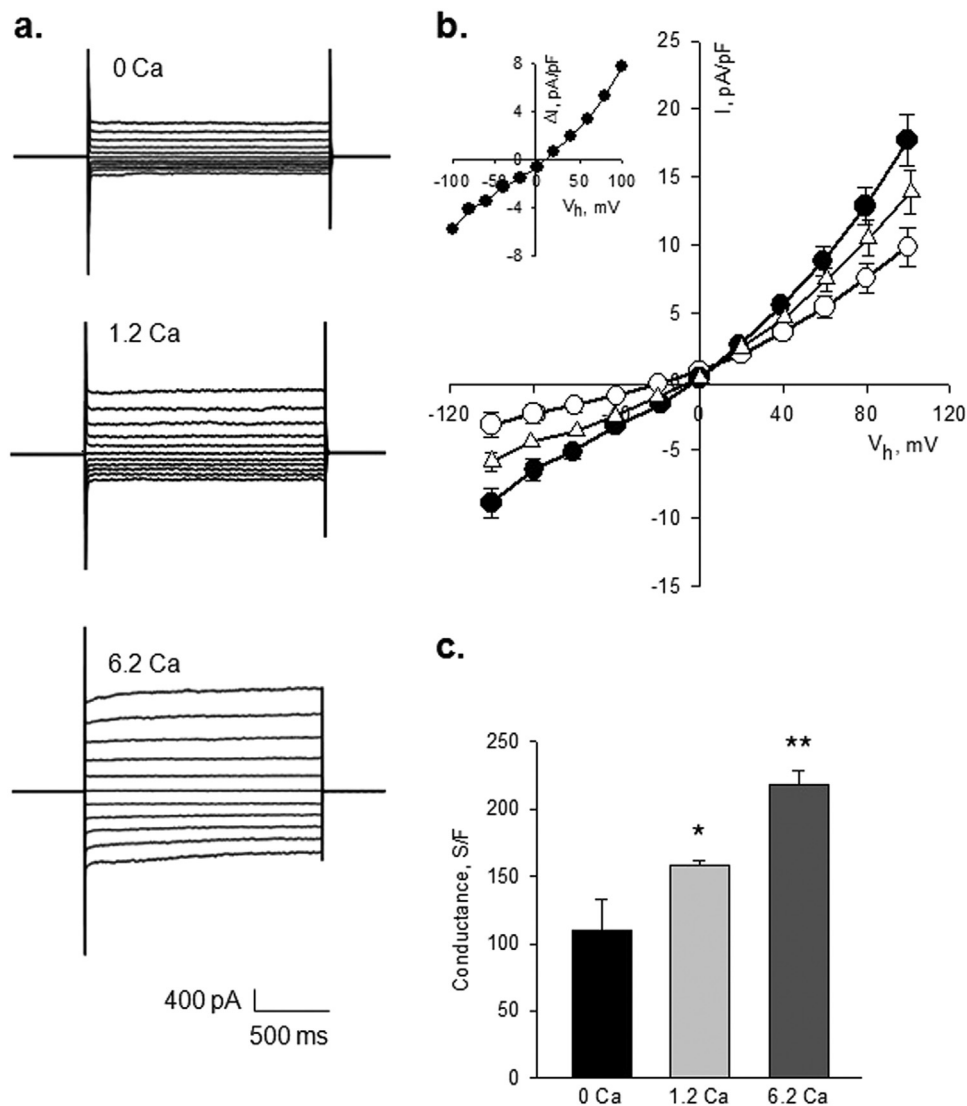


**Fig. 1.** Effect of external  $\text{Ca}^{2+}$  on the whole cell conductance of LLC-PK1 cells. (a). Representative whole cell currents of wild type LLC-PK1 cells in the absence (0 Ca), or the presence of 1.2 and 6.2 mM external  $\text{Ca}^{2+}$ . Data were obtained by voltage clamping with 20 mV-steps between  $\pm 100$  mV from a holding potential of zero mV. (b). Mean current-to-voltage relationships obtained in 0 Ca (open circles,  $n=6$ ), 1.2 Ca (open triangles,  $n=24$ ), and 6.2 Ca (filled circles,  $n=17$ ). Values are the mean  $\pm$  SEM of their respective experiments. The inset shows the 6.2 Ca-activated component of whole cell current. (c). Bar graph showing outwardly directed whole cell conductance for different external  $\text{Ca}^{2+}$  conditions as indicated in the graph. Asterisks indicate statistical significance ( $p < 0.01$ ) from each other.

### 3. Results

#### 3.1. Effect of external $\text{Ca}^{2+}$ on the whole cell conductance of LLC-PK1 cells

To explore the effect of external  $\text{Ca}^{2+}$  on the whole cell conductance of cultured wild type LLC-PK1 cells, whole cell voltage clamping was applied to isolated cells by stepping voltages between  $\pm 100$  mV from a holding potential of zero mV. In the presence of 1.2 Ca, the whole cell conductance was  $158 \pm 4.0$  S/F ( $n=24$ , Fig. 1a–c), with a reversal potential ( $V_{\text{rev}}$ ) of  $-7.56 \pm 1.02$  mV. The basal whole cell conductance measured over the linear voltage range (+60 to +100 mV) of LLC-PK1 cells in the absence of external  $\text{Ca}^{2+}$  (0 Ca, Fig. 1b and c) however, was 43.3% lower,  $110 \pm 23$  S/F ( $n=7$ ). The reversal potential ( $V_{\text{rev}}$ ) of the current-to-voltage relationship was  $-16.8 \pm 0.53$  mV. Conversely, in the 6.2 Ca solution, the whole cell conductance further increased to  $218 \pm 11$  S/F,  $n=17$  (Fig. 1b and c), which was 97.9% higher than in 0 Ca ( $p < 0.01$ ), with a  $12.9 \pm 0.81$  mV shift in  $V_{\text{rev}}$  ( $-3.89$  mV vs.  $-16.8$  mV, respectively). To test whether the increased whole cell conductance in 6.2 Ca was osmotically-induced, cells were exposed to

a 1.2 Ca solution supplemented with 15 mM sucrose. The sucrose-challenged cells had remarkably different current-to-voltage relationships presenting an increased inwardly rectifying conductance (data not shown). The outwardly directed conductance however, was  $145 \pm 2.0$  S/F,  $n=15$ , which was indistinguishable from the control value ( $p < 0.3$ ). Further, the  $V_{\text{rev}}$  under these conditions was  $21.4 \pm 0.21$  mV, which was also different from those observed in either 6.2 Ca or 1.2 Ca solutions. Thus, the osmotic activation was independent respect to the modulating effect of external  $\text{Ca}^{2+}$ .

#### 3.2. Effect of PC2 inhibition on the whole cell conductance of LLC-PK1 cells

To determine whether plasma membrane-associated PC2 contributed to the whole cell conductance of wild type LLC-PK1 cells, cells were dialyzed with a 1:200 dilution of the anti-PC2 antibody raised against the carboxy terminus of the channel protein, which has been shown to inhibit PC2 single channel activity [3,10,29]. Intracellular dialysis with the active antibody in cells exposed to 1.2 Ca decreased the whole cell conductance by 45.3% ( $178 \pm 4.4$  S/F,  $n=12$  vs.  $81.0 \pm$

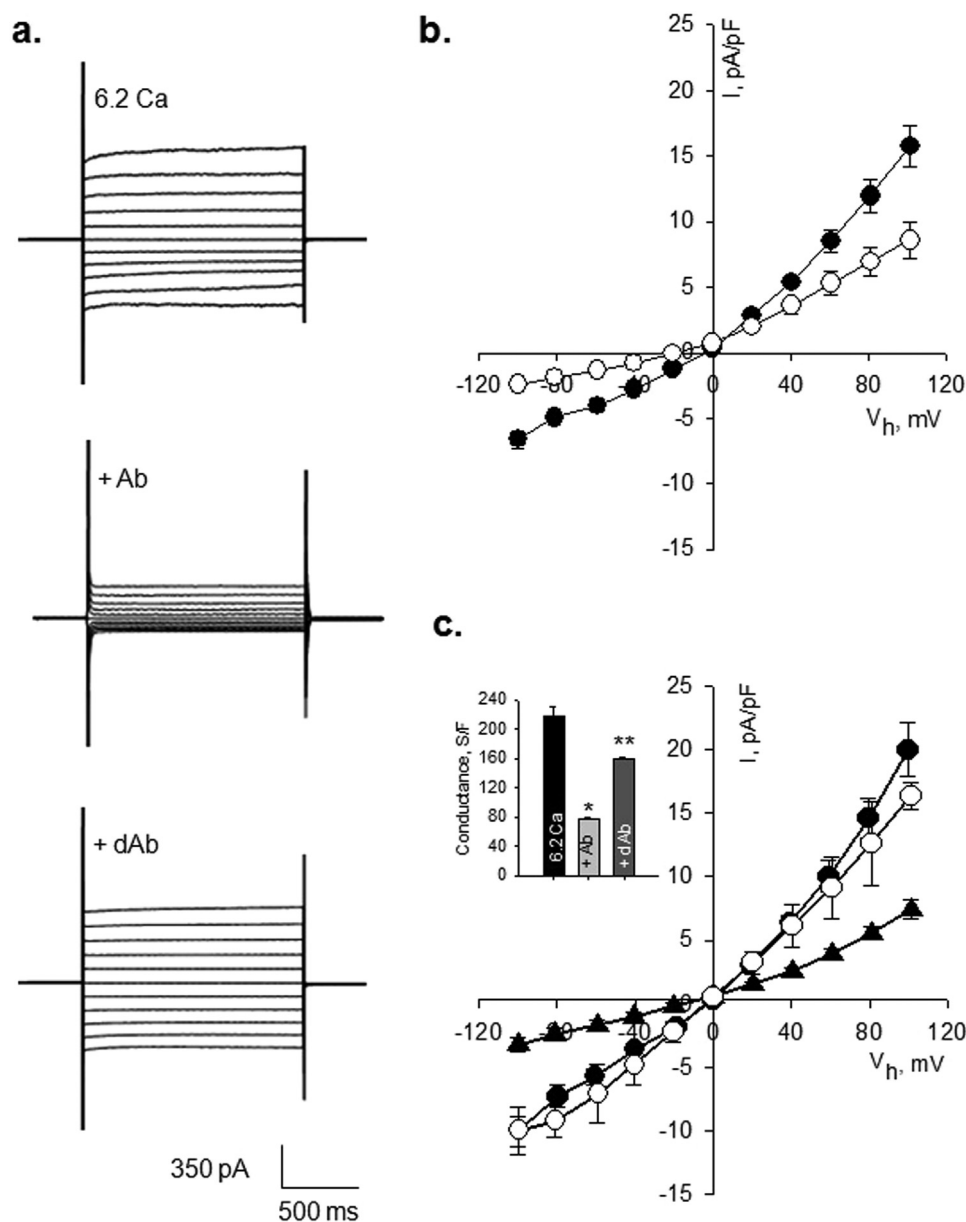


**Fig. 2.** Effect of anti-PC2 antibody on high  $Ca^{2+}$ -induced whole-cell conductance of LLC-PK1 cells. (a). Representative whole cell currents of wild type LLC-PK1 cells in 6.2 Ca, in the presence of either native (+Ab), or boil-denatured (+dAb) anti-PC2 antibody. Data were obtained by voltage clamping as indicated in Fig. 1. (b). Comparison of current-to-voltage relationships obtained in 1.2 Ca conditions (filled circles) and those dialyzed with native anti-PC2 antibody (1:200, open circles). Values are the mean  $\pm$  SEM of 24, and 10 experiments, respectively. (c). Current-to-voltage relationships obtained in 6.2 mM  $Ca^{2+}$  (filled circles), in the presence of either native (filled triangles), or boil-denatured anti-PC2 antibody (1:200, open circles). Data are the mean  $\pm$  SEM of 17, 8, and 10 experiments, respectively. Inset: Bar graph showing outwardly directed whole cell conductance values for different conditions as indicated in the graph. Asterisks indicate statistical significance ( $p < 0.001$ ), for control vs. +Ab (one asterisk), and between +Ab and +dAb (two asterisks), respectively.

1.6 S/F,  $n=5$ ,  $p < 0.001$ , Fig. 2b). In the presence of 6.2 Ca, the whole cell conductance of cells dialyzed with active antibody was  $76 \pm 3.0$  S/F,  $n=8$ , which was 65% lower than in the absence of anti-PC2 antibody (Fig. 2a and c, see above,  $p < 0.001$ ). The effect was also observed by a change in the  $V_{rev}$  to  $-15.0 \pm 3.6$  mV. The same experiment, conducted with boil-denatured antibody however, rendered a whole cell conductance of  $158 \pm 3$  S/F,  $n=10$ , which was only 27.6% lower than in the absence of antibody, and  $V_{rev}$  of  $-3.84 \pm 0.3$  mV (Fig. 2a–c). As expected, intracellular dialysis with active antibody to cells osmotically-challenged with sucrose (15 mM), had no effect on either the outwardly rectifying whole cell conductance ( $121 \pm 8$  S/F) or the  $V_{rev}$  ( $13.3 \pm 2.7$  mV,  $n=7$ ), confirming the lack of PC2 osmotic activation (data not shown).

### 3.3. Down-regulation of PKD2 gene expression by siRNA treatment of LLC-PK1 cells

To confirm the involvement of a functional PC2 in the external  $Ca^{2+}$ -stimulated whole-cell currents of wild type LLC-PK1 cells, the PKD2 gene expression was suppressed by siRNA treatment. The siPKD2 was designed to target exon 3 of the porcine PKD2 gene, as recently reported [37]. LLC-PK1 cells were transfected with an aliquot of 0.15  $\mu$ M of siRNA (see Section 2), and whole cell currents were obtained in cells after 72 h-treatment. Transfection efficiency and single cell detection were assessed by fluorescent siRNA uptake, suggesting that small synthetic siRNAs were readily taken up by LLC-PK1 cells, as previously reported [37]. In 6.2 Ca conditions, the siRNA-treated LLC-PK1 cells showed a 59% reduction in the whole cell currents, as compared to their own controls, Irss-treated cells ( $88 \pm 1$

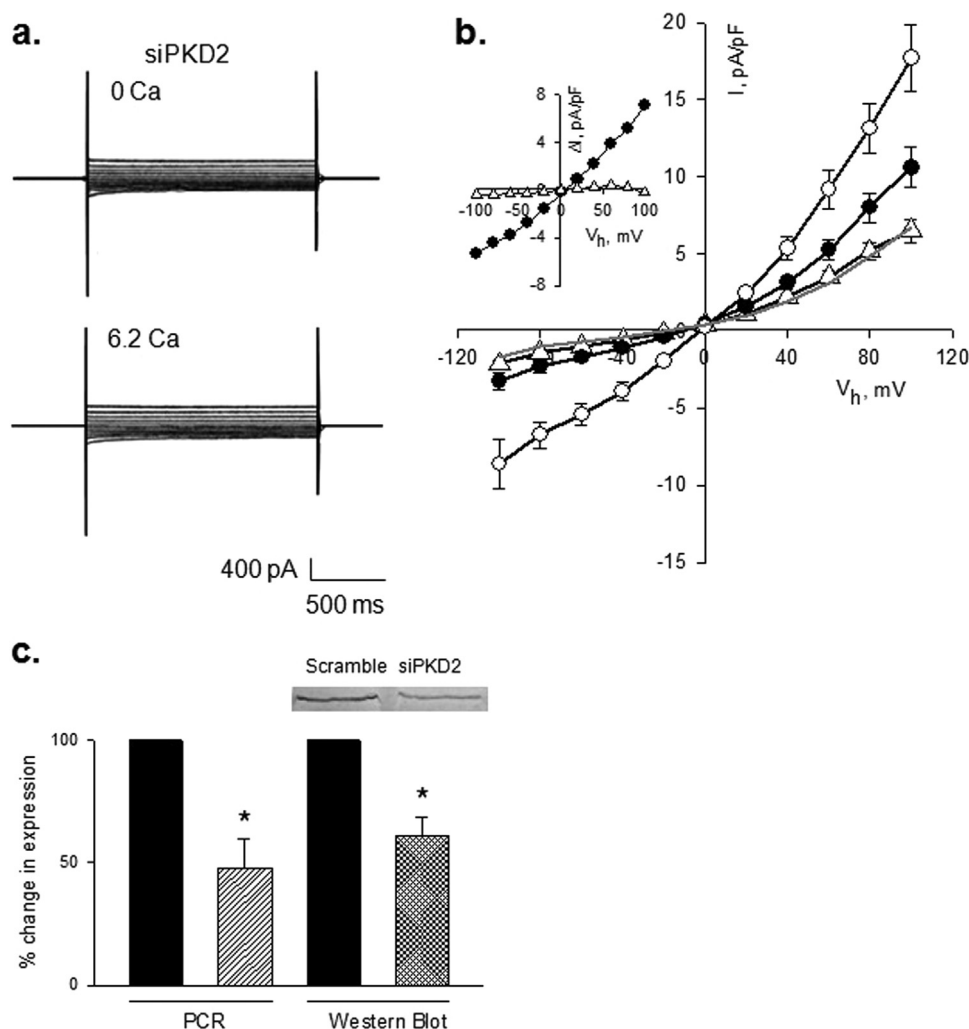


**Fig. 3.** Effect of PC2 silencing on the whole-cell conductance of LLC-PK1 cells. (a). Representative whole cell currents of siRNA PC2 silenced LLC-PK1 cells either in 0 Ca or 6.2 Ca. Data were obtained by voltage clamping as indicated in Fig. 1, and representative of 26 and 30 experiments, respectively. (b). Mean current-to-voltage relationships obtained in siRNA silenced cells in 0 Ca (gray line) or 6.2 Ca (open triangles). Please note that values almost entirely overlap. Mean current-to-voltage relationships are also shown for the Irss-treated cells in 0 Ca (filled circles,  $n=21$ ), and 6.2 Ca (open circles,  $n=30$ ). The Inset shows the 6.2 Ca-activated whole-cell currents in Irss-treated cells (filled circles) and siRNA silencing (open triangles) conditions, respectively. (c). Bar graph showing mean decrease in PKD2 gene product assessed by qPCR after 72 h-treatment with siRNA ( $n=3$ , Left), and Western blotting conducted with scrambled and specific PC2 siRNA ( $n=4$ , Right). A Western blot is shown on top. Asterisks indicate statistical significance ( $p < 0.01$ ) obtained by unpaired t-test.

S/F,  $n=30$  vs.  $213 \pm 8.4$  S/F,  $n=30$ ,  $p < 0.0001$ , respectively, Fig. 3a and b) with  $V_{\text{rev}} -5.42 \pm 0.5$  mV, and  $-14.4 \pm 0.3$  mV, respectively. This reduction was in close agreement with the inhibition observed by intracellular dialysis with active anti-PC2 antibody, but somewhat lower than that in 0 Ca, suggesting that even in the absence of external Ca, there is a background PC2 current. Under 0 Ca conditions, PC2 silencing was also effective in reducing by 37% ( $84.6 \pm 4.3$  S/F,  $n=23$ , vs.  $134 \pm 2.4$  S/F,  $n=21$ ,  $p < 0.0001$ , for the PC2 siRNA and Irss, with  $V_{\text{rev}} -19.1 \pm 0.8$  mV and  $-10.3 \pm 0.9$  mV, respectively). The specific PKD2 gene expression knock-down was confirmed by harvesting siRNA-transfected LLC-PK1 cells for RNA assay 72 h post-transfection. Real-time quantitative PCR was conducted and normalized to the  $\beta 2\text{MG}$  housekeeping gene. The results showed an average  $47.9 \pm 12\%$ ,  $n=3$  decrease of PKD2 mRNA level (Fig. 3c). The silencing efficiency was confirmed by Western blotting of equal amounts of lytic cell extracts from scramble- and specific siRNA-treated cells, separated by 10% SDS-PAGE gel electrophoresis, transfer to nitrocellulose membrane, and immunodetection with the primary anti PC2 antibody (1:500, Santa Cruz Biotechnology) at 4 °C, subsequently identified by the horseradish peroxidase reaction (1:500, Promega) with specific labeling was detected by treatment with diaminobenzidine (DAB, Sigma Aldrich). Western blots showed a rather similar reduction of

$39 \pm 7.2\%$  ( $n=4$ , Fig. 3c) to the value obtained by qPCR.

#### 3.4. Effect of external $\text{Ca}^{2+}$ on PC2 distribution

To assess whether the external  $\text{Ca}^{2+}$  concentration regulated PC2 cellular localization, subconfluent monolayers of LLC-PK1 cells were exposed for 5–10 min to saline solutions containing different external  $\text{Ca}^{2+}$  concentrations. Cells were then fixed, permeabilized, and immunolabeled with anti-PC2 antibody, FITC-phalloidin to label actin structures, and DAPI to identify cell nuclei. Cells incubated in the 0 Ca solution showed largely diffuse intracellular PC2 localization mostly in the perinuclear region (Fig. 4a). Cortical actin cytoskeleton was prominent in delimiting cell shape, and thus a surrogate of the membrane-associated regions, used as areas of interest. Punctate PC2 labeling (see Section 2, Fig. 4a, white arrows) was also observed within these regions, in agreement with previous findings [44]. Particle analysis of this punctate labeling was statistically similar in the 0 Ca and 1.2 Ca conditions ( $0.43 \pm 0.19$  AU/cell,  $n=74$  vs.  $0.79 \pm 0.21$  AU/cell,  $n=88$ ,  $p < 0.1$ ), but was dramatically increased in cells exposed to 6.2 Ca (310%) respect to control conditions ( $3.24 \pm 0.75$  AU/cell  $n=77$ ,  $p < 0.001$ , Fig. 4a and c). Osmotically-stressed cells by addition of sucrose (15 mM) showed no PC2 re-localization, in agreement with the

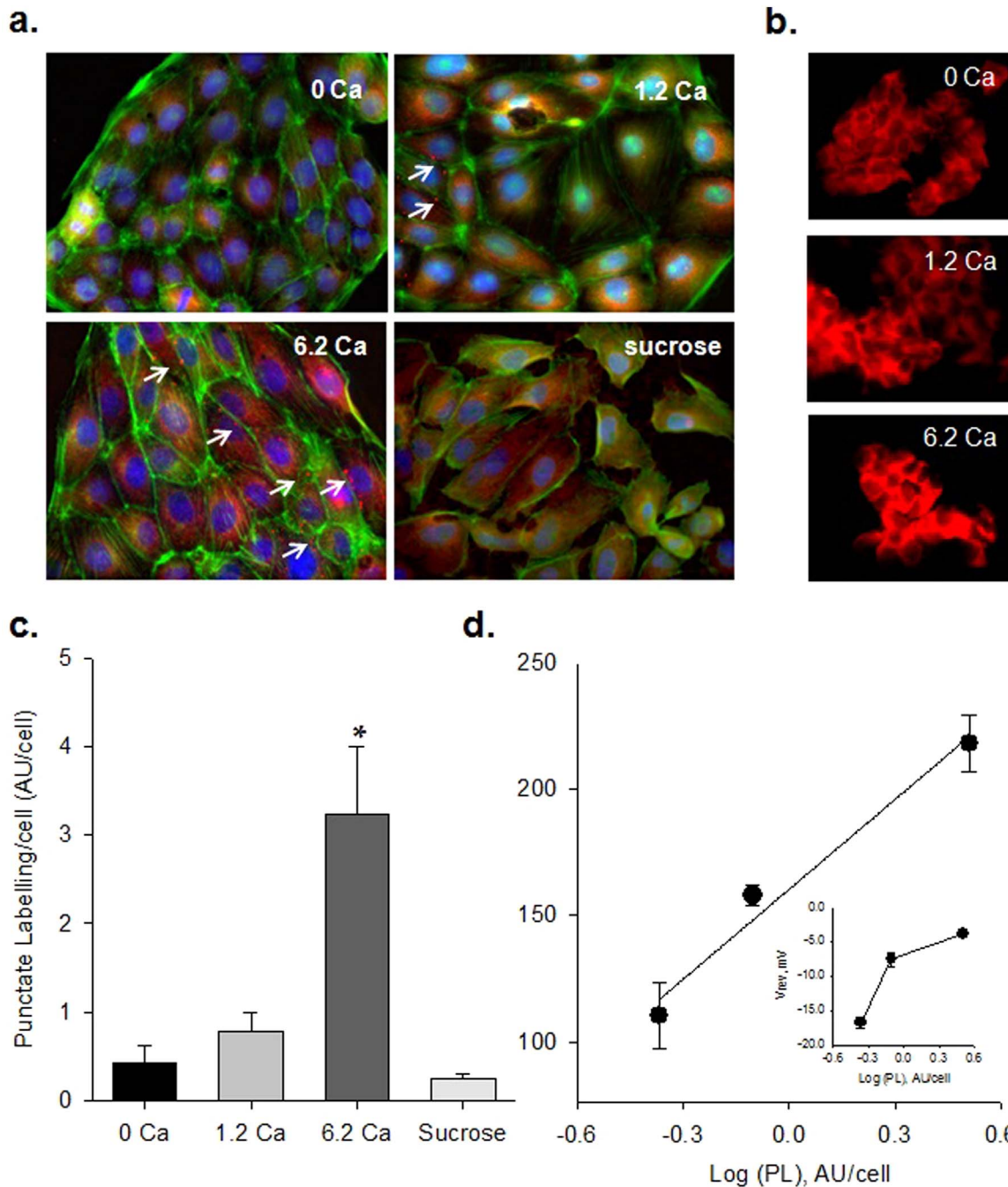


**Fig. 4.** Effect of external  $\text{Ca}^{2+}$  and sucrose on PC2 localization. (a). Partially confluent LLC-PK1 cells were exposed for 5–10 min to either different external  $\text{Ca}^{2+}$  concentrations (as indicated), or 15 mM sucrose. Cells were stained with anti-PC2 antibody (Cy3, Red), FITC-phalloidin (Green), and DAPI (Blue) ( $\times 40$ ). Exposure to 6.2 Ca showed redistribution of punctate PC2 labeling (shown with white arrows) compared to other external  $\text{Ca}^{2+}$  conditions. Cells exposed to added sucrose showed no PC2 redistribution. (b). External epitope PC2 antibody labeling ( $\text{Ab}^{\text{exep}}$ ) of non-permeabilized partially confluent LLC-PK1 cells in the presence of various external  $\text{Ca}^{2+}$  concentrations (as indicated). There is a marked change in external PC2 labeling at different  $\text{Ca}^{2+}$  concentrations. (c). Bar graph showing mean punctate plasma membrane PC2 per cell (see Section 2) for different conditions as indicated above. Data are the mean  $\pm$  SEM for 88, 74, 77, and 66, for 0, 1.2, and 6.2 Ca, and sucrose conditions, respectively. Asterisk indicates statistical significance ( $p < 0.001$ ) respect to 0 and 1.2 Ca conditions. (d). Correlation between punctate PC2 labeling quantification and whole cell conductance for different external  $\text{Ca}^{2+}$  concentrations. Inset shows the Log-Linear correlation between the PC2 labeling and the  $V_{\text{rev}}$  of the current-to-voltage relationships. Values are the mean  $\pm$  SEM of 7, 24, and 17 experiments, respectively. All points were statistically different from each other ( $p < 0.05$ ). (For interpretation of the references to color in this figure legend, the reader is referred to the web version of this article.)

lack of a PC2-associated whole cell conductance under these conditions. The effect of external  $\text{Ca}^{2+}$  on the modulation of plasma membrane PC2 expression was confirmed by surface labeling in non-permeabilized cells exposed to PC2- $\text{Ab}^{\text{exep}}$ . Surface labeling of PC2 with this antibody increased with the external  $\text{Ca}^{2+}$  concentration (Fig. 4b).

### 3.5. Correlation between membrane-associated PC2 and whole cell conductance

To explore whether PC2 redistribution contributed to the whole-cell conductance of LLC-PK1 cells, punctate PC2 labeling was correlated with the whole cell conductance for the different external  $\text{Ca}^{2+}$  conditions. The two parameters were strongly correlated (Fig. 4d), suggesting that external  $\text{Ca}^{2+}$  regulates, at least in part, the expression

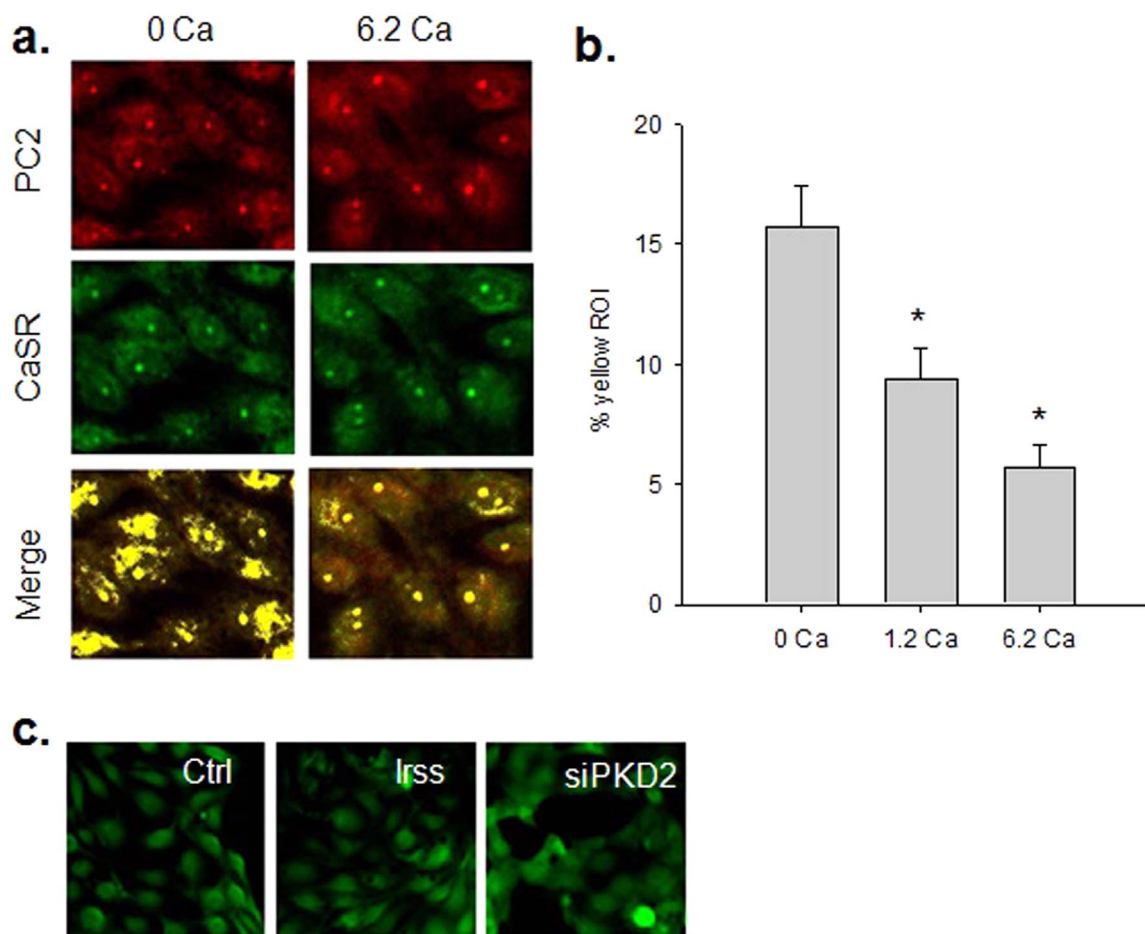


**Fig. 5.** Effect of external  $\text{Ca}^{2+}$  on CaSR and PC2 colocalization. Partially confluent wild type LLC-PK1 cells were exposed for 5–10 min, to saline containing different external  $\text{Ca}^{2+}$  concentrations prior to fixation. (a). Fixed cells were stained with anti- PC2 (Cy3, Red), and anti-CaSR antibodies (FITC, Green) ( $\times 20$ ). ROI for each experimental condition were segmented and threshold adjusted for each channel (Red and Green), and then quantified for a co-label channel (Merged, Yellow). (b). Bar graph showing ROI (%) for different external  $\text{Ca}^{2+}$  conditions, as indicated. Data are representative of 126 cells taken from three different experiments (42 cells per experiment) under each experimental condition. Asterisk indicates statistical significance respect to 0  $\text{Ca}^{2+}$  condition ( $p < 0.05$ ). (c). Cells were also treated for PC2 antisense conditions, and incubated in 0 Ca, as reported. The panels show CaSR labeling for control cells (Ctrl), scramble siRNA (Irrs), and the specific PC2 antisense probe (siPKD2), respectively. (For interpretation of the references to color in this figure legend, the reader is referred to the web version of this article.)

of functional plasma membrane PC2, and thus the whole cell conductance. This phenomenon was further supported by the inverse correlation between external  $\text{Ca}^{2+}$  concentration, and the observed change in  $V_{\text{rev}}$  of the activated conductance, consistent with a non-selective cation current (Fig. 4d, Inset), and thus more depolarizing reversal potentials.

### 3.6. Colocalization of the $\text{Ca}^{2+}$ -sensing receptor with PC2

The effect of high external  $\text{Ca}^{2+}$  on the whole cell conductance of LLC-PK1 cells would be consistent with the presence and activation of a CaSR [12,20], which is present in various regions of the nephron [31]. To confirm the possibility that external  $\text{Ca}^{2+}$  regulates a CaSR in wild type LLC-PK1 cells, small confluent cell monolayers were exposed for 5–10 min to different external  $\text{Ca}^{2+}$  concentrations, which were then fixed and colabeled with both CaSR and PC2 antibodies. The images were processed as described in Section 2, to quantify regions of colocalization. CaSR showed strong cytoplasmic labeling and PC2 colocalization at low and high external  $\text{Ca}^{2+}$  concentrations (Fig. 5a). It was observed however, that high external  $\text{Ca}^{2+}$  induced the dissociation between the colocalized proteins (Fig. 5a and b). CaSR labeling however, was not correlated with the expression of PC2 (Fig. 5c).

### 3.7. Effect of CaSR agonists on the whole cell conductance of LLC-PK1 cells

To confirm that a functional CaSR is implicated in the PC2 activation of the whole cell currents, other CaSR agonists were tested in the absence of external  $\text{Ca}^{2+}$ . Addition of the calcimimetic CaSR agonist R-568 (5  $\mu\text{M}$ ), increased the whole cell conductance of control cells by 64% ( $118 \pm 5.0$  S/F,  $n=7$ , vs.  $194 \pm 7.2$  S/F,  $n=6$ , Fig. 6a and b). This phenomenon was entirely blocked in PC2 silenced cells (Fig. 6a and b) ( $59.4 \pm 1.5$  S/F,  $n=7$  vs.  $62.2 \pm 4.8$  S/F,  $n=6$ ,  $p=0.56$ , and  $V_{\text{rev}} -13.0 \pm 0.2$  mV, and  $-12.6 \pm 0.2$  mV, for controls and R-568-treated cells, respectively). The stimulatory effect was also observed by addition of spermine (2 mM), known to activate CaSR [6], which increased the whole cell conductance by 94% ( $229 \pm 10.3$  S/F,  $n=15$ , vs.  $118 \pm 5$  S/F,  $n=7$ ,  $p < 0.0001$ , Fig. 6b). CaSR activation was also tested in the 1.2 Ca condition in LLC-PK1 cells exposed to the aminoglycoside gentamicin, known to activate CaSR [22]. Addition of gentamicin (250  $\mu\text{g}/\text{ml}$ ) to the bathing solution elicited a rapid and significant 76% increase in the whole cell conductance ( $278 \pm 8.0$  S/F,  $n=7$ , vs.  $158 \pm 3$  S/F,  $n=24$ ,  $p < 0.01$ , Fig. 7a and b), which was accompanied by a small, not significant 2.52 mV shift in  $V_{\text{rev}}$  ( $-5.04$  mV to  $-7.56$  mV, respectively). The stimulatory effect of gentamicin was entirely blunted by intracellular dialysis with ketamine (1  $\mu\text{g}/\text{ml}$ ) ( $99 \pm 8$  S/F,  $n=12$ , and  $V_{\text{rev}} -10.6$  mV, Fig. 7d), known to inhibit the CaSR [16,20]. In the absence of gentamicin, however, ketamine only decreased 8.56% the



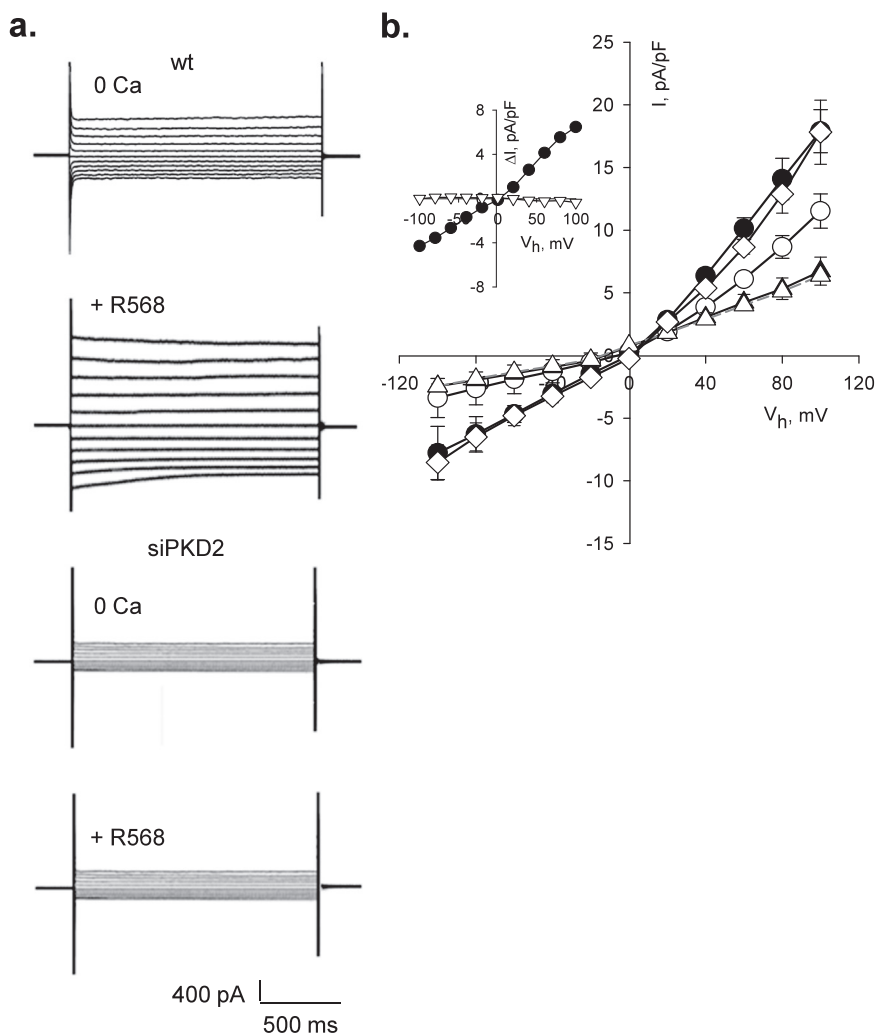


**Fig. 6.** Effect of calcimimetic CaSR agonist R-568 on the whole-cell conductance of LLC-PK1 cells. a. Representative whole cell currents of wild type LLC-PK1 cells either in the absence, or the presence of R-568 (5  $\mu$ M), and similar examples after siRNA PC2 silencing (siPKD2). All currents were obtained under  $\text{Ca}^{2+}$ -free conditions (0 Ca). Data were obtained by voltage clamping with 20 mV-steps between  $\pm 100$  mV from a holding potential of zero mV. (b). Mean current-to-voltage relationships for wild type cells in 0 Ca before (open circles,  $n=7$ ) and after addition of R-568 (filled circles,  $n=6$ ), as well as PC2 silenced cells in the absence (open triangles,  $n=11$ ) or presence (filled triangles,  $n=6$ ) of the drug. Current-to-voltage relationships were also obtained with another CaSR agonist, spermine (2 mM), with similar results (open rhomboids,  $n=15$ ). Values are the mean  $\pm$  SEM of their respective experiments. Inset shows the R-568-activated whole-cell currents under control (filled circles) and siRNA silencing (open triangles) conditions, respectively.

whole cell conductance to  $144 \pm 1$  S/F,  $n=12$ , which was largely similar to the control value in 1.2 Ca (data not shown). The contribution of plasma membrane PC2 to the CaSR-modulated whole cell conductance was confirmed by intracellular dialysis with active anti-PC2 antibody, which largely decreased (60.6%,  $p < 0.001$ ) the gentamicin-stimulated whole cell conductance ( $110 \pm 2$  S/F,  $n=6$ , Fig. 7c).

#### 4. Conclusions

The data in the present study demonstrate that PC2 is normally expressed in the plasma membrane of wild type LLC-PK1 renal epithelial cells, where it makes a significant contribution to the whole cell conductance. This background activity responds to the external  $\text{Ca}^{2+}$  concentration, such that it is almost absent under  $\text{Ca}^{2+}$ -free conditions, and conversely, it is magnified by higher external  $\text{Ca}^{2+}$  concentrations. Previous studies determined that PC2 itself does not interact with external  $\text{Ca}^{2+}$ , suggesting PC2-interacting partners in this regulation [3]. Thus, external  $\text{Ca}^{2+}$  modulates the whole cell conductance of wild type LLC-PK1 renal epithelial cells by regulating PC2-associated currents. Actually, the stimulatory effect of high external  $\text{Ca}^{2+}$  on the PC2 currents was associated with both, an increase of the PC2-contributed whole cell conductance, and the location of the PC2

channel protein in the plasma membrane. The functional contribution of endogenous PC2 in wild type LLC-PK1 cells to the increased whole cell conductance in high external  $\text{Ca}^{2+}$  is supported by the fact that intracellular dialysis with active, but not boil-denatured anti-PC2 antibody elicited a complete inhibition of this stimulatory effect. This inhibition was further supported by the knock-down expression of the PKD2 gene by siRNA silencing, as previously reported [37]. Quantitative PCR and Western blot analyses showed that the siRNA maneuver achieved about a 50% inhibition of the gene product, also in agreement with a previous report [37]. This reduction in the gene product expression elicited the complete inhibition of the external  $\text{Ca}^{2+}$ -stimulated currents. However, the whole cell conductance from siRNA-treated cells was lower than to that obtained under  $\text{Ca}^{2+}$ -free conditions, suggesting a basal, external  $\text{Ca}^{2+}$ -unrelated PC2 channel contribution.

The modulating effect of high external  $\text{Ca}^{2+}$  on the whole cell conductance was consistent with the stimulation of the  $\text{Ca}^{2+}$ -sensing receptor, CaSR, whose presence was supported by immunocytochemical labeling. CaSR activation was also elicited by CaSR agonists, including spermine [6,35] and the calcimimetic agonist R-568 [1,26] under  $\text{Ca}^{2+}$ -free conditions, and gentamicin [41,42] in normal  $\text{Ca}^{2+}$ . Further support for the CaSR-mediated regulation of PC2 was attained

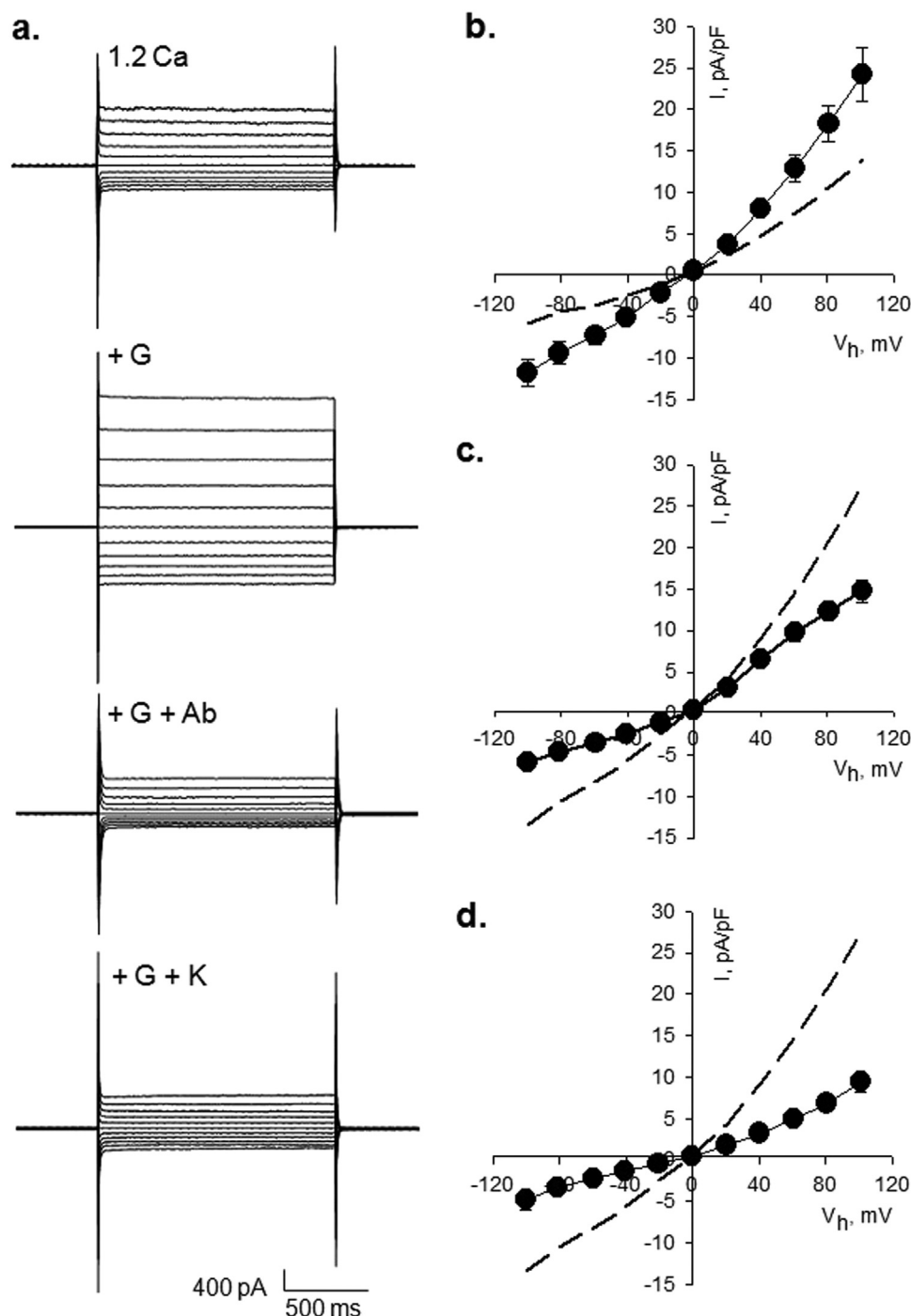


**Fig. 7.** Effect of CaSR modulation on the whole-cell conductance of LLC-PK1 cells. LLC-PK1 cells were voltage-clamped as for control conditions, in the presence of 1.2 Ca. (a). Representative tracings before (1.2 Ca) and after (+G) addition of the CaSR agonist gentamicin (250  $\mu\text{g}/\text{ml}$ ). Gentamicin-activated whole-cell currents were abolished by intracellular dialysis with anti-PC2 antibody (+G + Ab), and the CaSR antagonist, ketamine (+G + K). b. Current-to-voltage relationships in normal  $\text{Ca}^{2+}$  after addition of gentamicin (filled circles). Data are the mean  $\pm$  SEM for 7 experiments. The dashed line represents the control conductance in 1.2 Ca, as reference. (c). Gentamicin induces whole cell currents, in the absence (dashed line) but not in the presence of anti-PC2 antibody (1:200), filled circles. Data are the mean  $\pm$  SEM for 8 experiments. (d). Gentamicin whole cell currents (dashed line) in the presence of intracellular ketamine (1  $\mu\text{g}/\text{ml}$ ), filled circles. Data are the mean  $\pm$  SEM of 12 experiments.

by inhibition of the high  $\text{Ca}^{2+}$ -stimulated cation currents by intracellular dialysis with ketamine. This drug is a well-established anaesthetic associated with its ability to block NMDA receptors. In fact, ketamine exhibits an inhibitory effect on a wide variety of ion channels, and other molecular effects (for a review, see [33]). Ketamine has been associated with a decrease in intracellular  $\text{Ca}^{2+}$  in different cell models [16,43], which may be associated with inhibition of the  $\text{Ca}^{2+}$  sensing receptor, instead of changes in the release of intracellular  $\text{Ca}^{2+}$  [16]. The nature of the inhibitory effect on the PC2-mediated currents is currently

unknown, but the possible targets include inhibition of the channel itself, or the CaSR signaling pathway, including the receptor itself, the associated G proteins, and/or the phospholipid metabolites thereof, which will require further investigation.

Interestingly, co-localization of intracellular CaSR and PC2 was most prominent in cells exposed to low  $\text{Ca}^{2+}$ , and largely reduced in high  $\text{Ca}^{2+}$ , which would be consistent with the delivery of more available channel protein to the plasma membrane. Although the nature of this putative molecular complex remains presently undefined,

it is tempting to postulate that a CaSR-PC2 interaction may likely extend to the plasma membrane that would help explain the effect of external  $\text{Ca}^{2+}$  on the PC2-mediated whole cell currents. One possible scenario for the functional interaction between both proteins may entail the high external  $\text{Ca}^{2+}$ -elicited disassociation of the complex rendering an increased plasma membrane PC2 labeling and function under these conditions. This is in agreement with the fact that in normal  $\text{Ca}^{2+}$ , there is a background PC2 current.

The CaSR is a member of the GPCR superfamily, which couples to both  $G_q$  and  $G_i$  to elicit both activation of phospholipase and the subsequent mobilization of intracellular  $\text{Ca}^{2+}$ , as well as proteins that lower intracellular cAMP and inhibit associated signaling events [8]. CaSR is expressed in various nephron segments, including the apical membrane of the proximal tubule [31], where luminal  $\text{Ca}^{2+}$  and the calcimimetic agent R-568, modified  $\text{Na}^+$ -dependent proton secretion and fluid reabsorption [4]. CaSR activation either by hypercalcemia or mutations, results in clinically significant salt and water wasting, reaching severe volume depletion and hypotension [13]. Although the molecular steps linking CaSR activation to PC2 stimulation remain to be defined, our results are consistent with a mechanism entailing both the regulation of PC2 protein trafficking as well as plasma membrane PC2 channel activity. This is in agreement with previous evidence showing that CaSR interacts with, and inactivates the inwardly rectifying epithelial  $\text{K}^+$  channel, Kir4.1 [5], which contributes to the basolateral  $\text{K}^+$  conductance in the distal nephron. Our present data suggest that CaSR regulation of PC2 channel function may bear a direct role in the  $\text{Ca}^{2+}$  influx in renal epithelial cells, and/or the regulation of the resting potential, expected of TRP channels [17]. This is in agreement with our findings indicating that an increase in PC2-mediated whole-cell currents were always associated with a shift in reversal potential towards a more depolarizing value, which is consistent with monovalent cation non-selectivity. It is interesting to note, however, that Torres' group failed to observe an effect of the calcimimetic CaSR agonist R-568 in the development of cysts in two genetic models of kidney disease [40]. Their study showed no significant effect on cyst growth in either animal model, despite the fact that R-568 had pharmacologic effects on renal function and mineral metabolism [42]. Thus, the hypercalciuric effect of the drug was hypothesized as mediated by CaSR activation in the thick ascending limb of Henle and distal convoluted tubule [38,39], which was necessary for  $\text{K}^+$  recycling during Na-K-2Cl cotransporter activation, and passive paracellular reabsorption of  $\text{Ca}^{2+}$ . The present findings are relevant in this context, as PC2 may help modulate ionic homeostasis of both  $\text{K}^+$  and  $\text{Ca}^{2+}$ , in renal epithelial cells.

To date, little is known about the kind of external signals that trigger PC2 activation and/or regulation in the plasma membrane and the contribution endogenous plasma membrane PC2 makes to the basal conductance of renal epithelial cells. Previous studies by Ma et al. [19] showed that PC2 over-expression enhanced the EGF-induced whole-cell conductance of LLC-PK1 cells. To what extent this phenomenon could be entirely ascribed to a normal PC2 function remains to be determined. The present data in wild type LLC-PK1 cells indicate that blocking of endogenous PC2 function in normal  $\text{Ca}^{2+}$  (1.2 mM), either by dialysis with the anti-PC2 antibody or by gene product silencing, render a whole cell conductance that was lower than the one observed under  $\text{Ca}^{2+}$ -free conditions. This finding suggests that a basal level of PC2 activity occurs during normal cell function, even in the absence of extracellular  $\text{Ca}^{2+}$ . The effect of different  $\text{Ca}^{2+}$  concentrations, the shape of the resulting current-to-voltage relationships, and their respective changes in reversal potential are all consistent with the expected contribution of PC2 to a non-selective cation conductance, as originally reported [9]. In their study, Ma et al. [19] concluded that the EGF-activated currents in transfected cells were mediated by PC2. However, less than 5% of the total transfected PC2 reached the plasma membrane, which the authors speculated might be related to the fact that PC2 would require co-factors such as PC1 for targeting that cell

location [19]. Our data suggest instead a strong correlation between plasma membrane PC2 and external  $\text{Ca}^{2+}$ -modulated whole cell currents, raising the issue that high external  $\text{Ca}^{2+}$ , and other CaSR-activating maneuvers, may be almost entirely explained by activation of this channel protein.

To conclude, the present data are consistent with the presence of, and regulation by, the  $\text{Ca}^{2+}$ -sensing receptor, of PC2-associated channel currents in LLC-PK1 cells. Wild type LLC-PK1 cells responded to changes in external  $\text{Ca}^{2+}$  with the redistribution and stimulation of plasma membrane PC2, which is mediated by the  $\text{Ca}^{2+}$ -sensing receptor. The data further indicate that changes in endogenous plasma membrane PC2 makes a relevant contribution to electrodiffusional non-selective cation transport, eliciting a novel regulatory response to  $\text{Ca}^{2+}$  signals in renal epithelial cells.

## Acknowledgements

This work was partially supported by NIDDK grant 1R01DK077079-01A2 (HFC), and PICT 2012 #1559 MinCyT, Argentina, to HFC. MRC, PLP, MS and HFC are members of the National Research Council of Argentina (CONICET). DCM and GS were visiting graduate students from the School of Medicine, Mendoza, Argentina. We are grateful to Drs. Fernando Pieckenstein for the kind gift of spermine-tetrahydrochloride, and Ana Clara Casadoumeq and Dr. Cecilia Villa Etchegoyen for excellent technical support. XQD and KS would like to thank Dr. Patrick MacDonald for his support and generosity in allowing use of instrumentation and reagents in his laboratory.

## References

- [1] M. Bonomini, A. Giardinelli, C. Morabito, S. Di Silvestre, M. Di Cesare, N. Di Pietro, V. Sirolli, G. Formoso, L. Amoroso, M.A. Mariggio, A. Pandolfi, Calcimimetic R-568 and its enantiomer S-568 increase nitric oxide release in human endothelial cells, *PLoS ONE* 7 (1) (2012) e30682.
- [2] Y. Cai, Y. Maeda, A. Cedzich, V.E. Torres, G. Wu, T. Hayashi, T. Mochizuki, J.H. Park, R. Witzgall, S. Somlo, Identification and characterization of polycystin-2, the PKD2 gene product, *J. Biol. Chem.* 274 (1999) 28557–28565.
- [3] M.R. Cantero, H.F. Cantiello, Calcium transport and local pool regulate polycystin-2 (TRPP2) function in human syncytiotrophoblast, *Biophys. J.* 105 (2013) 365–375.
- [4] G. Capasso, P.J. Geibel, S. Damiano, P. Jaeger, W.G. Richards, J.P. Geibel, The calcium sensing receptor modulates fluid reabsorption and acid secretion in the proximal tubule, *Kidney Int.* 84 (2013) 277–284.
- [5] S.K. Cha, C. Huang, Y. Ding, X. Qi, C.-L. Huang, R.T. Miller, Calcium-sensing receptor decreases cell surface expression of the inwardly rectifying  $\text{K}^+$  channel Kir4.1, *J. Biol. Chem.* 286 (2011) 1828–1835.
- [6] S.X. Cheng, J.P. Geibel, S.C. Hebert, Extracellular polyamines regulate fluid secretion in rat colonic crypts via the extracellular calcium-sensing receptor, *Gastroenterology* 126 (2004) 148–158.
- [7] L. Foggenteiner, A.P. Bevan, R. Thomas, N. Coleman, C. Boulter, J. Bradley, O. Ibragimov-Beskrovnaia, K. Klinger, R. Sandford, Cellular and subcellular distribution of polycystin-2, the protein product of the PKD2 gene, *J. Am. Soc. Nephrol.* 11 (2000) 814–827.
- [8] A. Gerbino, W.C. Ruder, S. Curci, T. Pozzan, M. Zaccolo, A.M. Hofer, Termination of cAMP signals by  $\text{Ca}^{2+}$  and  $G_{\alpha i}$  via extracellular  $\text{Ca}^{2+}$  sensors: a link to intracellular  $\text{Ca}^{2+}$  oscillations, *J. Cell Biol.* 171 (2005) 303–312.
- [9] A. Giamarchi, F. Padilla, B. Coste, M. Raoux, M. Crest, E. Honore, P. Delmas, The versatile nature of the calcium-permeable cation channel TRPP2, *EMBO Rep.* 7 (2006) 787–793.
- [10] S. González-Perrett, K. Kim, C. Ibarra, A.E. Damiano, E. Zotta, M. Batelli, P.C. Harris, I.L. Reisin, M.A. Arnaout, H.F. Cantiello, Polycystin-2, the protein mutated in autosomal dominant polycystic kidney disease (ADPKD), is a  $\text{Ca}^{2+}$ -permeable nonselective cation channel, *Proc. Natl. Acad. Sci. USA* 98 (2001) 1182–1187.
- [11] C. Hajmirle, M. Ferdaoussi, G. Plummer, A.F. Spigelman, K. Lai, J.E. Manning Fox, P.E. MacDonald, SUMOylation protects against IL-1 $\beta$ -induced apoptosis in INS-1 832/13 cells and human islets, *Am. J. Physiol. Endocrinol. Metab.* 307 (2014) E664–E673.
- [12] A.M. Hofer, E.M. Brown, Extracellular calcium sensing and signalling, *Nat. Rev. Mol. Cell Biol.* 4 (2003) 530–538.
- [13] C. Huang, R.T. Miller, Novel Ca receptor signaling pathways for control of renal ion transport, *Curr. Opin. Nephrol. Hypertens.* 19 (2010) 106–112.
- [14] M. Köttgen, G. Walz, Subcellular localization and trafficking of polycystins, *Pflü"g. Arch.* 451 (2005) 286–293.
- [15] P. Koulen, Y. Cai, L. Geng, Y. Maeda, S. Nishimura, R. Witzgall, B.E. Ehrlich,

- S. Somlo, Polycystin-2 is an intracellular calcium release channel, *Nat. Cell Biol.* 4 (2002) 191–197.
- [16] A. Kudoh, A. Matsuki, Ketamine inhibits inositol 1, 4, 5-trisphosphate production depending on the extracellular  $\text{Ca}^{2+}$  concentration in neonatal rat cardiomyocytes, *Anesth. Analg.* 89 (1999) 1417–1422.
- [17] S. Lev, B. Minke, Constitutive activity of TRP channels: methods for measuring the activity and its outcome, *Methods Enzymol.* 484 (2010) 591–612.
- [18] Y. Luo, P.M. Vassilev, X. Li, Y. Kawanabe, J. Zhou, Native polycystin 2 functions as a plasma membrane  $\text{Ca}^{2+}$ -permeable cation channel in renal epithelia, *Mol. Cell Biol.* 23 (2003) 2600–2607.
- [19] R. Ma, W.P. Li, D. Rundle, J. Kong, H.I. Akbarali, L. Tsiokas, PKD2 functions as an epidermal growth factor-activated plasma membrane channel, *Mol. Cell Biol.* 25 (2005) 8285–8298.
- [20] A.L. Magno, B.K. Ward, T. Ratajczak, The calcium-sensing receptor: a molecular perspective, *Endocr. Rev.* 32 (2011) 3–30.
- [21] T. Mochizuki, G. Wu, T. Hayashi, S.L. Xenophontos, B. Veldhuisen, J.J. Saris, D.M. Reynolds, Y. Cai, P.A. Gabow, A. Pierides, W.J. Kimberling, M.H. Breuning, C.C. Deltas, D.J. Peters, S. Somlo, PKD2, a gene for polycystic kidney disease that encodes an integral membrane protein, *Science* 272 (1996) 1339–1342.
- [22] G. Molostvov, S. James, S. Fletcher, J. Bennett, H. Lehnert, R. Bland, D. Zehnder, Extracellular calcium-sensing receptor is functionally expressed in human artery, *Am. J. Physiol. Ren. Physiol.* 293 (2007) F946–F955.
- [23] C. Montell, Physiology, phylogeny, and functions of the TRP superfamily of cation channels, *Sci. STKE* 90 (2001) re1.
- [24] S.M. Nauli, F.J. Alenghat, Y. Luo, E. Williams, P.M. Vassilev, X. Li, A.E. Elia, W. Lu, E.M. Brown, S.J. Quinn, D.E. Ingber, J. Zhou, Polycystins 1 and 2 mediate mechanosensation in the primary cilium of kidney cells, *Nat. Genet.* 33 (2003) 129–137.
- [25] A.C. Ong, C.J. Ward, R.J. Butler, S. Biddolph, C. Bowker, R. Torra, Y. Pei, P.C. Harris, Coordinate expression of the autosomal dominant polycystic kidney disease proteins, polycystin-2 and polycystin-1, in normal and cystic tissue, *Am. J. Pathol.* 154 (1999) 1721–1729.
- [26] C. Pipino, P. Di Tomo, D. Mandatori, E. Cianci, P. Lanuti, M.B. Cutrona, L. Penolazzi, L. Pierdomenico, E. Lambertini, I. Antonucci, V. Sirolli, M. Bonomini, M. Romano, R. Piva, M. Marchisio, A. Pandolfi, Calcium sensing receptor activation by calcimimetic R-568 in human amniotic fluid mesenchymal stem cells: correlation with osteogenic differentiation, *Stem Cells Dev.* 23 (2014) 2959–2971.
- [27] A.J. Ramos, M.R. Cantero, P. Zhang, M.K. Raychowdhury, A. Green, D. MacPhee, H.F. Cantiello, Morphological and electrical properties of human trophoblast choriocarcinoma, BeWo cells, *Placenta* 29 (2008) 492–502.
- [28] M.K. Raychowdhury, C. Ibarra, A. Damiano, G.R. Jackson Jr, P.R. Smith, M. McLaughlin, A.G. Prat, D.A. Ausiello, A.S. Lader, H.F. Cantiello, Characterization of  $\text{Na}^{+}$ -permeable cation channels in LLC-PK1 renal epithelial cells, *J. Biol. Chem.* 279 (2004) 20137–20146.
- [29] M.K. Raychowdhury, M. Mc Laughlin, A.J. Ramos, N. Montalbetti, R. Bouley, D.A. Ausiello, H.F. Cantiello, Characterization of single channel currents from primary cilia of renal epithelial cells, *J. Biol. Chem.* 280 (2005) 34718–34722.
- [30] M.K. Raychowdhury, A.J. Ramos, P. Zhang, M. McLaughlin, X.Q. Dai, X.Z. Chen, N. Montalbetti, M.R. Cantero, D.A. Ausiello, H.F. Cantiello, Vasopressin receptor-mediated functional signaling pathway in primary cilia of renal epithelial cells, *Am. J. Physiol.* 296 (2009) F87–F97.
- [31] D. Riccardi, A.E. Hall, N. Chattopadhyay, J.Z. Xu, E.M. Brown, S.C. Hebert, Localization of the extracellular  $\text{Ca}^{2+}$ /polyvalent cation-sensing protein in rat kidney, *Am. J. Physiol. Ren. Physiol.* 274 (1998) F611–F622.
- [32] V. Singla, J.F. Reiter, The primary cilium as the cell's antenna: signaling at a sensory organelle, *Science* 313 (2006) 629–633.
- [33] J. Sleight, M. Harvey, L. Voss, B. Denny, Ketamine – more mechanisms of action than just NMDA blockade, *Trends Anaesth. Crit. Care* 4 (2014) 76–81.
- [34] G.W. Snedecor, W.G. Cochran, *Statistical Methods*, 6th ed., Iowa State Univ. Press, Ames IA, 1973.
- [35] P.E. Squires, Non- $\text{Ca}^{2+}$ -homeostatic functions of the extracellular  $\text{Ca}^{2+}$ -sensing receptor (CaR) in endocrine tissues, *J. Endocrinol.* 165 (2000) 173–177.
- [36] P.M. Vassilev, L. Guo, X.Z. Chen, Y. Segal, J.B. Peng, N. Basora, H. Babakhanlou, G. Cruger, M. Kanazirska, Ye Cp, E.M. Brown, M.A. Hediger, J. Zhou, Polycystin-2 is a novel cation channel implicated in defective intracellular  $\text{Ca}^{2+}$  homeostasis in polycystic kidney disease, *Biochem. Biophys. Res. Commun.* 282 (2001) 341–350.
- [37] Q. Wang, H. Yin, J. He, J. Ye, F. Ding, S. Wang, X. Hu, Q. Meng, N. Li, cDNA cloning of porcine PKD2 gene and RNA interference in LLC-PK1 cells, *Gene* 476 (2011) 38–45.
- [38] W.H. Wang, M. Lu, M. Balazy, S.C. Hebert, Phospholipase A2 is involved in mediating the effect of extracellular  $\text{Ca}^{2+}$  on apical  $\text{K}^{+}$  channels in rat TAL, *Am. J. Physiol. Ren. Physiol.* 273 (1997) F421–F429.
- [39] W.H. Wang, M. Lu, S.C. Hebert, Cytochrome P-450 metabolites mediate extracellular  $\text{Ca}^{2+}$ -induced inhibition of apical  $\text{K}^{+}$  channels in the TAL, *Am. J. Physiol. Cell Physiol.* 271 (1996) C103–C111.
- [40] X. Wang, P.C. Harris, S. Somlo, D. Batlle, V.E. Torres, Effect of calcium-sensing receptor activation in models of autosomal recessive or dominant polycystic kidney disease, *Nephrol. Dial. Transpl.* 24 (2009) 526–534.
- [41] D.T. Ward, D. Maldonado-Pérez, L. Hollins, D. Riccardi, Aminoglycosides induce acute cell signaling and chronic cell death in renal cells that express the calcium-sensing receptor, *J. Am. Soc. Nephrol.* 16 (2005) 1236–1244.
- [42] D.T. Ward, D. Riccardi, Renal physiology of the extracellular calcium-sensing receptor, *Pflug. Arch.* 445 (2002) 169–176.
- [43] Y.Q. Wu, T. Liang, H. Huang, Y.Z. Zhu, P.P. Zhao, C.M. Xu, L. Liu, X.T. Shi, Y. Hu, L. Huang, C.H. Zhou, Ketamine inhibits proliferation of neural stem cell from neonatal rat hippocampus in vitro, *Cell Physiol. Biochem.* 34 (2014) 1792–1801.
- [44] B.K. Yoder, X. Hou, L.M. Guay-Woodford, The polycystic kidney disease proteins, polycystin-1, polycystin-2, polaris, and cystin, are co-localized in renal cilia, *J. Am. Soc. Nephrol.* 13 (2002) 2508–2516.